

# UNCLASSIFIED

AD NUMBER
ADB280825
NEW LIMITATION CHANGE
TO Approved for public release, distribution unlimited
FROM Distribution: Further dissemination only as directed by OSRD, Washington, DC 20330, Sep 1943; or higher DoD authority.
AUTHORITY
OSRD, per DTIC Form 55, dtd 14 Nov 2002.

THIS PAGE IS UNCLASSIFIED

NDRC  
A-218 2532

~~CONFIDENTIAL~~

A.P.M. (C) 334.9/295  
28 Sep 43

Confidential  
A-218  
NDRC

NATIONAL DEFENSE RESEARCH COMMITTEE

ARMOR AND ORDNANCE REPORT NO. A-218 (OSRD NO. 1868)

DIVISION 2

Classification Extension to 10 years

*Unclassified*

Authority: 101 CFR 101-11.6

OSRD List 14 JF.

THIRD PROGRESS REPORT

ON

PLASTIC DEFORMATION OF STEEL UNDER HIGH PRESSURE

Sep 43

by

DISTRIBUTION STATEMENT F:

P. W. Bridgman

Further dissemination only as directed by

OSRD, Wash., DC 20330  
or higher DoD authority.

This document contains information affecting the national defense of the United States within the meaning of the Espionage Act, U.S.C., 50; 31 and 32. Its transmission or the revelation of its contents in any manner to an unauthorized person is prohibited by law.

Reproduced From  
Best Available Copy

20020701 251

Copy No. 50

~~CONFIDENTIAL~~

~~CONFIDENTIAL~~

U

NATIONAL DEFENSE RESEARCH COMMITTEE  
ARMOR AND ORDNANCE REPORT NO. A-218 (OSRD NO. 1868)  
DIVISION 2

THIRD PROGRESS REPORT  
ON  
PLASTIC DEFORMATION OF STEEL UNDER HIGH PRESSURE

by  
P. W. Bridgman

Approved on September 23, 1943  
for submission to the Division Chief

P. W. Bridgman  
P. W. Bridgman, Consultant  
Division 2

Merit P. White  
Merit P. White, Secretary  
Division 2

Approved on September 28, 1943  
for submission to the Committee

John E. Burchard  
John E. Burchard, Chief  
Division 2  
Structural Defense and Offense

RESEARCH INFORMATION BRANCH  
ORDNANCE RESEARCH CENTER  
ABERDEEN PROVING GROUND  
MARYLAND

~~CONFIDENTIAL~~

U

## Preface

The work described in this report is pertinent to the project designated by the Navy Department Liaison Officer as NO-11 and to Division 2 project P2-302.

This work was carried out and reported by Harvard University as part of its performance under Contract ONRsr-201.

### Initial distribution of copies of the report

Nos. 1 to 25, inclusive, to the Office of the Secretary of the Committee for distribution in the usual manner;

No. 26 to R. C. Tolman, Vice Chairman, NDRC;

No. 27 to R. Adams, Member, NDRC

No. 28 to F. B. Jewett, Member, NDRC;

No. 29 to J. E. Burchard, Chief, Division 2;

No. 30 to W. Bleakney, Deputy Chief, Division 2;

No. 31 to W. F. Davidson, Office of the Chairman, NDRC;

No. 32 to R. A. Beth, Member, Division 2;

No. 33 to H. L. Bowman, Member, Division 2;

No. 34 to C. W. Curtis, Member, Division 2;

No. 35 to C. W. Lampson, Member, Division 2;

No. 36 to W. E. Lawson, Member, Division 2;

No. 37 to H. P. Robertson, Mission London;

No. 38 to F. Seitz, Member, Division 2;

No. 39 to A. H. Taub, Member, Division 2;

No. 40 to E. B. Wilson, Jr. Member, Division 2;

Nos. 41 and 42 to R. J. Slutz, Technical Aide, Division 2;

No. 43 to Army Air Forces (Brig. Gen. B. W. Chidlaw);

Nos. 44 and 45 to Corps of Engineers (Col. J. H. Stratton, Lt. Col. F. S. Besson, Jr.);

No. 46 to Ordnance Department (Col. S. B. Ritchie);

No. 47 to H. P. White, Technical Aide, Division 2;

No. 48 to Corps of Engineers (Lt. Col. S. B. Smith);

No. 49 to Watertown Arsenal (Col. H. H. Zarnig);

No. 50 to Aberdeen Proving Ground (O. Veblen);

Nos. 51 and 52 to Bureau of Ordnance (Lt. Comdr. T. J. Flynn, A. Wertheimer);

No. 53 to U. S. Naval Proving Ground (Lt. Comdr. R. A. Sawyer);

No. 54 to David Taylor Model Basin (Capt. W. P. Roop);

No. 55 to Bureau of Ships (Lt. Comdr. R. W. Garanson);

No. 56 to Bureau of Yards and Docks (War Plans Officer);

No. 57 to U.S. Naval Research Laboratory (R. Gunn);

No. 58 to D. S. Clark, Consultant, Division 2;

No. 59 to A. Nadai, Consultant, Division 2;

No. 60 to P. W. Bridgman, Consultant, Division 2.

The NDRC technical reports section  
for armor and ordnance edited  
this report and prepared it for duplication.

## CONTENTS

	<u>Page</u>
Abstract .....	1
<u>Section</u>	
1. Introduction .....	1
2. Distribution of stress across the necked specimen .....	3
3. Relation between flow stress and natural strain .....	6
4. Detailed results and discussion .....	8
5. Conclusion .....	20

## List of Figures

<u>Figure</u>	<u>Page</u>
1. Two curves relating to the effects of necking in tension specimens .....	4
2,3. Corrected true stress at fracture and maximum pressure during pulling versus natural strain for plate 18A .....	15
4. Ratio of area of tensile fracture to area of neck versus maximum pressure during pulling for plate 18A .....	15
5,6. Corrected true stress at fracture and maximum pressure during pulling versus natural strain for plate 13F .....	16
7. Ratio of area of tensile fracture to area of neck versus maximum pressure during pulling for plate 13F .....	16
8,9. Corrected true stress at fracture and maximum pressure during pulling versus natural strain for plate 17F .....	17
10. Ratio of area of tensile fracture to area of neck versus maximum pressure during pulling for plate 17F .....	17

<u>Figure</u>		<u>Page</u>
11,12.	Corrected true stress at fracture and maximum pressure during pulling versus natural strain for plate 6X1 .....	18
13.	Ratio of area of tensile fracture to area of neck versus maximum pressure during pulling for plate 6X1 .....	18
14.	Double neck on a tension specimen from plate 17F .....	19
15.	Photograph that shows the method of sectioning a tension specimen .....	21
16-19.	Specimens from plate C14 broken in tension under atmospheric pressure; and under hydrostatic pressures of 4000, 10,100 and 15,800 kg/cm <sup>2</sup> .....	21,23

THIRD PROGRESS REPORT ON  
PLASTIC DEFORMATION OF STEEL UNDER HIGH PRESSURE

Abstract

Tests of the mechanical properties of steels under high hydrostatic pressure which were described in previous reports<sup>1,2/</sup> were continued, using four samples of armor plate of varying ballistic qualities. The conclusion, in accord with the results of other lines of investigation, is that ballistic behavior is closely associated with fairly obvious characteristics -- such as inhomogeneity, brittleness, and so forth -- which can be investigated by standard methods. The conclusions regarding strain hardening and conditions for fracture, given in the earlier reports, have been improved, but not essentially changed, by considering the true stress state in the neck of a tensile specimen.

1. Introduction

The present work constitutes an attempt to answer one of the original questions that was deemed important when this program was initiated, namely, whether by taking account of the properties of plate under pressure it might be possible to anticipate ballistic failure. The question was of interest because at that time there were many cases of obscure correlation between ballistic failure and the more usual physical properties; but it could not be answered in the two earlier reports<sup>1,2/</sup> because samples of plate which had failed to meet the ballistic tests were not then available.

In this report data are given for the effect of hydrostatic pressure on the tensile properties of four samples of armor plate.

---

1/ P. W. Bridgman, Plastic deformation of steel under high pressure, NDRC Report A-95 (OSRD No. 919).

2/ P. W. Bridgman, Second progress report on plastic deformation of steel under high pressure, NDRC Report A-162 (OSRD No. 1347).



Table I. Physical properties of the three new plates as reported by Doctor M. Gensamer of the Carnegie Institute of Technology.

Plate No.	Thickness (in.)	Ballistic Performance	Average Tensile Data				Average V-notch Charpy Impact Test**	
			Type Specimen*	Tensile Strength (10 <sup>3</sup> lb/in <sup>2</sup> )	Elongation (percent)	Reduction in Area (percent)	Temperature of Test (°C)	Energy (ft lb)
18A	1.5	Passed; 100 ft/sec above specification	Length	137	19	59	0	36
			Width	138	17	50	-40	25
			Thickness	135	12	31	-60	20
17F	1.5	Failed; back spall 2-3/16 × 3-7/8 in.	Length	131	20	61	0	34
			Width	130	14	41	-40	29
			Thickness	99	2	8	-60	21
13F	2	Failed; cracked through thickness of plate in a plane normal to the surface of the plate	Length	135	17	59	0	24
			Width	131	16	54	-40	15
			Thickness	126	10	21	-60	12

\* Length specimens taken parallel to direction of rolling, width specimens perpendicular to direction of rolling, thickness specimens perpendicular to face of plate.

\*\* Long axis of specimen taken perpendicular to direction of rolling, notch taken in thickness direction.

Partial data have already been presented for one of these plates<sup>3/</sup> but three of the plates are new. The particular significance of these three new plates is that other of their physical properties have already been examined elsewhere. Two of these plates had failed in the ballistic test.

The three new plates were supplied by Dr. M. Gensamer, of the Carnegie Institute of Technology, who provided a description of their physical properties.<sup>4/</sup> These are presented in Table I.

The measurements of the present report differ from those of the two earlier reports in that the effect of orientation in the plates was more carefully examined, tests being made on specimens cut in three mutually perpendicular directions: parallel to face and parallel to rolling (X-direction); parallel to face and perpendicular to rolling (Y-direction); and perpendicular to face (Z-direction). The fourth plate, designated 6X1 in the first report, was examined with respect to the strain-hardening curve and the effect of pressure on the character of the fracture, points that had received only inadequate consideration in the first report. The particular plate 6X1 was selected because previous experience had shown that it was of good homogeneity.

## 2. Distribution of stress across the necked specimen

The results presented here have been improved in one important respect in comparison with those of the two previous reports. It is known that the tension is not uniformly distributed across the neck of a tension specimen, and that this lack of uniformity will affect the value of the flow and rupture stresses calculated from tension experiments. Previously, there has been no satisfactory method of calculating the precise distribution of stress across the necked specimen, and in the absence of such precise knowledge it has been the custom to report the results in terms

---

<sup>3/</sup> Reference 1.

<sup>4/</sup> In two personal letters dated Dec. 23, 1942 and Aug. 3, 1943.

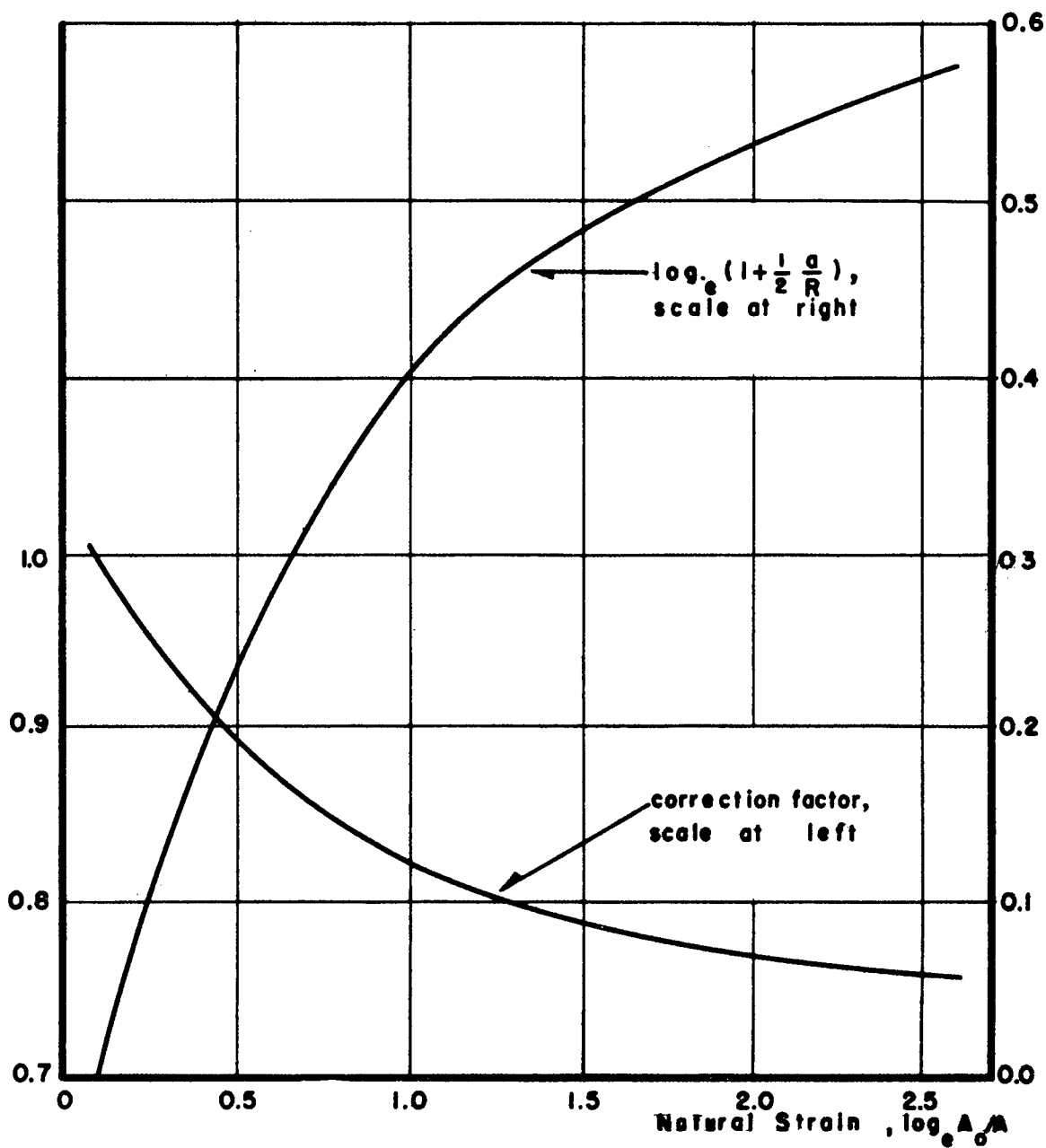


Fig.1. TWO CURVES RELATING TO THE EFFECTS OF NECKING IN TENSION SPECIMENS.

of the average tension across the neck. Under ordinary circumstances it was to be anticipated that the correction for lack of uniformity was not very serious; but with the abnormally large degree of necking which prevails in these experiments because of the great increase of ductility under hydrostatic pressure, the correction may be expected to become more important. Fortunately, since the publication of the first two reports, a method has been found for obtaining the precise distribution of stress across the neck and for evaluating the correction arising from lack of uniformity.<sup>5/</sup> The results given in the present report are corrected for this effect; in order to permit comparison with previous work, the uncorrected results are also given. In some cases, where the necking is extreme, the corrected stress of flow may be 75 percent of the uncorrected stress. So much of the results of the analysis as is necessary for present purposes is reproduced in the two curves of Fig. 1. One curve shows the correction factor in terms of the "natural" strain at the neck, that is,  $\log_e A_0/A$ , where  $A_0$  is the initial cross-sectional area and  $A$  is the final cross-sectional area; the other curve shows the factor by which may be calculated the hydrostatic tension on the axis generated by the necking. The detailed analysis evaluates these two factors in terms of the ratio of the radius of curvature of the contour at the neck to the radius of the neck, and not in terms of the natural strain at the neck. However, it is an empirical result, valid over a wide range of conditions, that to the degree of approximation of the present experiments the ratio of the two radii may be taken to be a universal function of the natural strain. By means of the curves of Fig. 1, the stresses given in the two first reports may be corrected. The effect of the correction is to diminish the tabulated flow and fracture stresses; the fraction by which these stresses are to be diminished is greater, the greater the reduction of area.

---

<sup>5/</sup> The detailed analysis is in course of publication by the American Society for Metals.

### 3. Relation between flow stress and natural strain

Application of the correction for necking does not alter the important result of the second report, that is, the true flow stress is a linear function of the natural strain. However, recognition of the existence of the correction alters the qualitative nature of the picture with regard to fracture. To show what the character of this change is it will be necessary to describe in further detail the results of the analysis.

Consider a tension specimen pulled under normal conditions in a testing machine at atmospheric pressure to such an amount that there is appreciable necking. At the neck there is a distribution of stress which may be analyzed into the sum of two distributions. The first is a tensile stress along the axis of the specimen and constant across the section of the neck; the second is a hydrostatic tension which vanishes at the outer surface of the neck and which increases to a maximum value on the axis according to a law that is given explicitly in the afore-mentioned paper. On the axis the hydrostatic tension is the product of  $\log_e(1 + \frac{1}{2} \frac{a}{R})$  and the constant tension, where  $a$  is the radius of the neck and  $R$  is the radius of curvature of the contour at the neck. If we represent the stresses in conventional cylindrical coordinates --  $z$  along the axis,  $r$  along the radius and  $\theta$  in the plane through the radius at right angles to the  $z$ -axis -- then the principal stresses are as follows:

At the outside surface

$$\hat{r}r = 0$$

$$\hat{\theta}\theta = 0$$

$$\hat{z}z = F$$

On the axis

$$\hat{r}r = F \log_e(1 + \frac{1}{2} \frac{a}{R})$$

$$\hat{\theta}\theta = F \log_e(1 + \frac{1}{2} \frac{a}{R})$$

$$\hat{z}z = F \log_e(1 + \frac{1}{2} \frac{a}{R}) + F$$

where  $F$  is determined by the condition that the integral of  $\hat{z}z$  across the section shall equal the applied tensile load.

In the region of plastic flow before rupture the specimen is flowing uniformly and the strain is constant across the narrowest

section of the neck. The rate of flow or the amount of strain hardening is assumed in the analysis to be independent of the hydrostatic component of the total stress, an assumption which is amply justified by experiment. Hence a strain hardening curve is to be constructed by plotting the simple tensile component  $\underline{F}$  against the natural strain at the neck, and this is also the strain-hardening curve if the total stress system is the sum of  $\underline{F}$  and a hydrostatic term. It is shown in the paper mentioned that  $\underline{F}$  is obtained by dividing the conventional average tensile stress -- that is, the total tensile load divided by the cross-sectional area at the neck -- by  $(1 + 2 \frac{R}{a}) \log_e (1 + \frac{1}{2} \frac{a}{R})$ . The reciprocal of this expression is the "correction factor" shown in Fig. 1.

Fracture, unlike plastic flow before fracture, does not occur uniformly across the neck but is initiated at a particular point on the axis, where the total stress system has a uniquely determined value. Now it is well established by experiment that fracture, unlike plastic flow, is strongly dependent on the hydrostatic component of the total stress system, the strain at fracture increasing greatly with superposed hydrostatic pressure. In order to characterize completely the conditions of fracture in a tensile test, three parameters should be given: the strain, the simple tensile component,  $\underline{F}$ , and the hydrostatic component,  $F \log_e (1 + \frac{1}{2} \frac{a}{R})$ . This complete specification could not be given before the correction for necking was known.

If the tensile test is made in a medium under hydrostatic pressure, then the complete stress system is the sum of three systems, the two just considered and the imposed hydrostatic pressure. This imposed hydrostatic pressure does not affect the flow parameters, and the strain hardening curve is still to be specified by giving  $\underline{F}$  as a function of the strain at the neck. The hydrostatic component of the stress at fracture is now, however, the hydrostatic tension arising from the necking, which is equal to  $F \log_e (1 + \frac{1}{2} \frac{a}{R})$ , minus the imposed hydrostatic pressure.

We pass now to a consideration of the actual measurements. The detailed arrangements of the experiments of this third report, including the dimensions of the specimens, were exactly like those in the second report,<sup>6/</sup>

#### 4. Detailed results and discussion

The results are summarized in Tables II to V and Figs. 2 to 14. As in the previous report, each entry or point in a diagram is a condensation of an entire curve, consisting of 10 to 20 readings of tensile load, hydrostatic pressure and extension. It is not necessary to reproduce the original curves in detail; the significant parameters of these curves are the data given here.

Most of the entries in the tables are self-explanatory. The "Corrected true stress at fracture" of column 9 is the same as the  $\bar{F}$  of Sec. 3. The "Hydrostatic tension on axis arising from necking" of column 10 is  $F \log_e (1 + \frac{1}{2} \frac{a}{R})$ . The "Net hydrostatic tension on axis" of column 11 is column 10 minus the maximum corresponding pressure of column 2. The "Net tension at fracture" of column 12 is column 9 plus column 11. The values listed in the tables for atmospheric pressure agree fairly well with the values reported by Gensamer, obtained under different experimental conditions.

(a) Relation between true stress at fracture and natural strain at the neck. -- These new results in the first place substantiate results previously found. Consider, for example, Figs. 2, 5, 8 and 11. In these the true stress at fracture, corrected for the nonuniformity of the stress distribution at the neck, appears to be a linear function of the natural strain at the neck at fracture. In the previous report the uncorrected true stress was also found to be such a linear function. All the test pieces of the present report were pulled to fracture; in previous work the tests were often not carried to fracture, and it was found that the stress-strain relation below fracture follows the same linear relation as that which represents the fractures. In other words, the corrected true stress at the neck, plotted against

---

<sup>6/</sup> Reference 2.

the running natural strain at the neck, moves along the straight lines of the figures as strain increases during the course of an experiment. Fracture is a catastrophe that suddenly terminates the experiment without the running point leaving the line or without any other warning. This means that the lines of Figs. 2, 5, 8 and 11 are essentially concerned with the phenomena of plastic flow and strain-hardening and not with fracture. This is emphasized further by reference to the effect of orientation.

(b) Dependence of strain-hardening and fracture phenomena on orientation. -- In Figs. 2, 5 and 8, the points for the three orientations all lie on the same lines independent of the orientation, which means that for a given natural strain the true stress and therefore the strain-hardening is independent of orientation. However, specimens with different orientations vary in their fracture phenomena. For example, the X-direction of plate 13F breaks under atmospheric pressure at a corrected true stress of 15,300 kg/cm<sup>2</sup>, whereas the corresponding fracture stress for the Z-direction is only 10,600 kg/cm<sup>2</sup>. Although fracture in the Z-direction occurs before fracture in the X-direction, up to the instant of fracture the stress-strain curves for the two directions have been identical. The natural strain at fracture for the X-direction is 0.936, and that for the Z-direction much less, only 0.275.

(c) Numerical parameters of the strain-hardening curves. -- The numerical parameters of the strain-hardening curves of the four different plates differ only slightly. We may take for these parameters (i) the value of the flow stress at a natural strain of 0.1, which is approximately the point where necking begins in a tension specimen, and (ii) the stress at a natural strain of 3.0. The latter parameter is probably the more significant of the two under the conditions of armor penetration because it indicates the resistance at high degrees of distortion. The stress at a natural strain of 0.1 for the plates 18A, 13F, 17F and 6X1 is, respectively, 12,500, 10,000, 10,400 and 7,000 kg/cm<sup>2</sup>, and the





**Table IV.** Summary of tension tests under pressure on plate 17F.

Column 1	Column 2	Column 3	Column 4	Column 5	Column 6	Column 7	Column 8	Column 9	Column 10	Column 11	Column 12	Column 13
Orientation of Specimen	Pressure Range (kg/cm <sup>2</sup> )	Ratio of Original Area to Final Area A <sub>0</sub> /A	Reduction of Area (percent)	Natural Strain at Fracture Loge (A <sub>0</sub> /A)	Average Stress on Original Area at Maximum Load (kg/cm <sup>2</sup> )	Average Stress on Original Area (kg/cm <sup>2</sup> )	True Stress at Fracture (kg/cm <sup>2</sup> )		Hydrostatic Tension on Axle Arising from Necking (kg/cm <sup>2</sup> )	Net Hydrostatic Tension on Axle (kg/cm <sup>2</sup> )	Net Tension at Fracture (kg/cm <sup>2</sup> )	Ratio of Area of Tensile Fracture to Total Area of Neck
							Uncorrected	Corrected				
X	Atmos.	2.74	63.5	1.008	9820	7250	12900	16100	6500	6500	22900	0.468
	5450	5.05	80.1	1.619	11000	4900	24900	19400	9900	2800	22200	.128
	7100											
	8800	13.15	92.5	2.576	11150	2550	33600	25100	15000	1300	26700	.000
	13700											
Y	Atmos.	1.87	46.6	0.625	10260	9610	18000	15500	4400	4400	20000	—
	Atmos.	2.19	54.3	.786	12740	10960	24000	20500	6800	6800	27300	0.438
	5200	2.02	50.6	.705	10750	8390	17000	14600	4500	-1700	12900	—
	6200											—
	8900	2.27	56.0	.820	10600	?	?	?				—
Z	Atmos.	1.06	6.1	0.062	10000	10000 ?	?	?				—
	Atmos.	1.27	21.6	.243	9800	9500	12100 ?	11500 ?				—
	5250											
	5950											
	8600											
	10900											

Too irregular for measurement

Too irregular for measurement

Table V. Summary of tension tests under pressure on plate 6X1 (X-direction). ✓

Column 1	Column 2	Column 3	Column 4	Column 5	Column 6	Column 7	Column 8	Column 9	Column 10	Column 11	Column 12	Column 13
X	Atmos.	2.93	66.0	1.075	9190	5760	16900	13800	5800	5800	19600	0.33
	1400	3.57	71.9	1.272	9700	5440	19300	15400	7100	5100	20500	.27
	2000											
	6200	8.38	88.6	2.126	9840	3250	27200	20800	11600	3400	24200	.09
	8200											
	8400											
	11000	11.94	91.7	2.430	10140	2100	25000	19000	11200	100	19100	.06
	8750											
	13900	19.85	95.2	2.988	10120	1740	34500	25800	15800	1900	27700	.03

corresponding stresses at a natural strain of 3.0 are 27,500, 25,800, 27,700 and 25,700 kg/cm<sup>2</sup>. These latter figures are so similar that very similar ballistic behavior of the four plates is to be expected, other things being equal. Included in the "other things being equal" is homogeneity.

(d) Increase of ductility with hydrostatic pressure. -- We now turn from a consideration of the phenomena of plastic flow to the phenomena of fracture. In the second report it was shown that the ductility, as measured by the natural strain at fracture, increases linearly with hydrostatic pressure. In Figs. 3, 6, 9 and 12, the pressure at which the specimen was pulled is plotted against the natural strain at fracture. There is much scattering of the points, indicative of the lack of homogeneity of the material, but within the limits of error, the relation again seems to be linear. The first three plates -- 18A, 13F, and 17F -- are arranged in order of increasing inhomogeneity. That this is the proper order is shown by the way in which the points are scattered. For plate 18A the points representing the X-, Y- and Z-orientations all lie on the same line within the limits of error. For plate 13F the points of the X- and Y-orientations are roughly on the same line, whereas those of the Z-orientation tend to lie on another line corresponding to easier fracture in this direction. Finally, for 17F the points are much more irregular; only the points for the X-direction tend to lie on a line at all; the points for the Y-direction are badly scattered, and for the Z-direction the results are so capricious that measurements could be made at all only for two out of four specimens tested. It happened that these two measurable specimens were those tested under atmospheric pressure.

(e) Principal stress components at fracture. -- Columns 11 and 12 of Tables II to V determine the principal stress components at fracture. In fact, both  $\hat{r}\hat{r}$  and  $\hat{\theta}\hat{\theta}$  have the value given in column 11 and  $\hat{z}\hat{z}$  has the value given in column 12. The three components could be plotted together in three dimensions to give

a fracture surface. When the stress in the substance attains a value corresponding to a point on the surface, fracture occurs. The strain at fracture is another parameter, varying from point to point of the surface. Special values of it are given in column 4.

In general, the stress components  $\hat{r}\hat{r}$  and  $\hat{\theta}\hat{\theta}$  shown in column 11 diminish with increasing hydrostatic pressure (column 2) or with increasing strain at fracture. One would expect a regular connection, but if column 11 is plotted against column 2 or 5, great irregularity will be found. Fracture data are always capricious, and the irregularity is enhanced here by the fact that column 11 is the small difference of nearly equal numbers. The greatest regularity is shown by the most homogeneous steel, 6X1. The fourth test on this plate is out of line with the others; this may be plausibly explained by premature fracture due to a flaw. If this point is discarded, the others are fairly regular. If now  $\hat{r}\hat{r}$  (or  $\hat{\theta}\hat{\theta}$ ) for 6X1 is plotted against  $\hat{z}\hat{z}$ , a straight line is obtained. This line may be extrapolated to the point where  $\hat{r}\hat{r} = \hat{z}\hat{z}$ ; it occurs at about 10,000 kg/cm<sup>2</sup>. The significance of the point of intersection is that here the total stress system which produces rupture reduces to a hydrostatic tension. This hydrostatic tension which produces rupture has often been called the cohesive strength; for plate 6X1 the cohesive strength thus appears to be about 10,000 kg/cm<sup>2</sup>.

We may obtain approximately the same result by another line of argument. The mean hydrostatic tension corresponding to any stress system is  $(\hat{r}\hat{r} + \hat{\theta}\hat{\theta} + \hat{z}\hat{z})/3$ . The mean hydrostatic tensions for the first, second, third and fifth tests on 6X1 are, respectively, 10,400, 10,200, 10,300 and 10,500 kg/cm<sup>2</sup>. These are constant, within limits of error -- an interesting result in itself, doubtless of significance. Now when fracture occurs under pure hydrostatic tension with no other stress component, the strain must vanish. Hence, if we plot the four tensions just calculated against the corresponding strains and extrapolate to

zero strain, the corresponding hydrostatic tension will be the cohesive strength. But since the four tensions are constant and hence independent of strain, the extrapolated value when strain vanishes is the same constant value, or approximately  $10,000 \text{ kg/cm}^2$ , checking with the result just obtained by another method. This figure for the cohesive strength is lower than would be estimated from previous speculations in the literature. The lowering of the figure is a result of the correction for necking.

(f) Character of the fracture. -- Finally, we consider the character of the fracture itself. In the second report it was shown that the cup and cone fracture which normally occurs under atmospheric pressure tends to disappear at high pressures, the area of the tensile part of the fracture -- that is, the flat bottom of the cup as distinguished from the sides where the fracture is on shear planes -- occupying a progressively smaller fraction of the total area of the neck, and vanishing altogether at pressures between  $15,000$  and  $20,000 \text{ kg/cm}^2$ . The last columns of Tables II to V and Figs. 4, 7, 10 and 13 show the fraction of the total area occupied by the tensile break as a function of the hydrostatic pressure during pulling. The result already found is substantiated; the ratio of the areas drops off linearly with increasing pressure, vanishing in the neighborhood of  $15,000 \text{ kg/cm}^2$ , a pressure above which the fracture is entirely along shear planes.

The greatest effects of difference of orientation and lack of homogeneity appear when one studies the character of the fracture. The X-direction for all plates -- that is, the direction parallel to the face and parallel to the direction of rolling -- permitted satisfactory measurements. The Y- and Z-directions for 18A also permitted such measurements, showing approximate homogeneity, whereas the Z-direction of plate 13F and both Y- and Z-directions of plate 17F in general gave such indefinite fractures that they could not be analyzed into a tensile and a shearing part. Plate 17F in particular gave highly abnormal fractures. Mention may be made especially of the specimen of 17F in the Z-direction

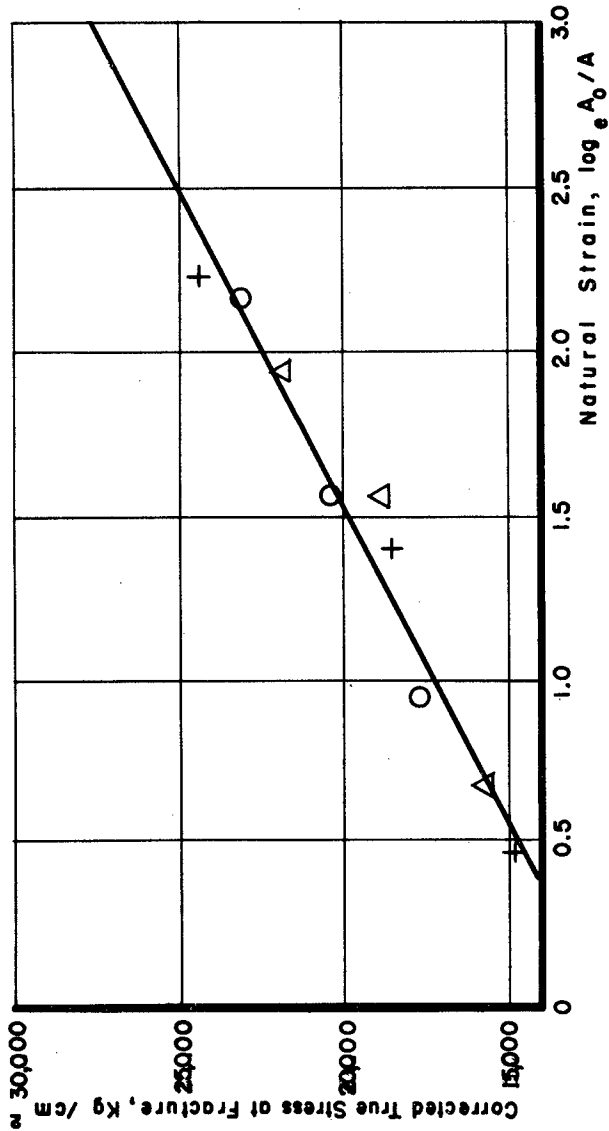


Fig. 2. PLATE 18A.

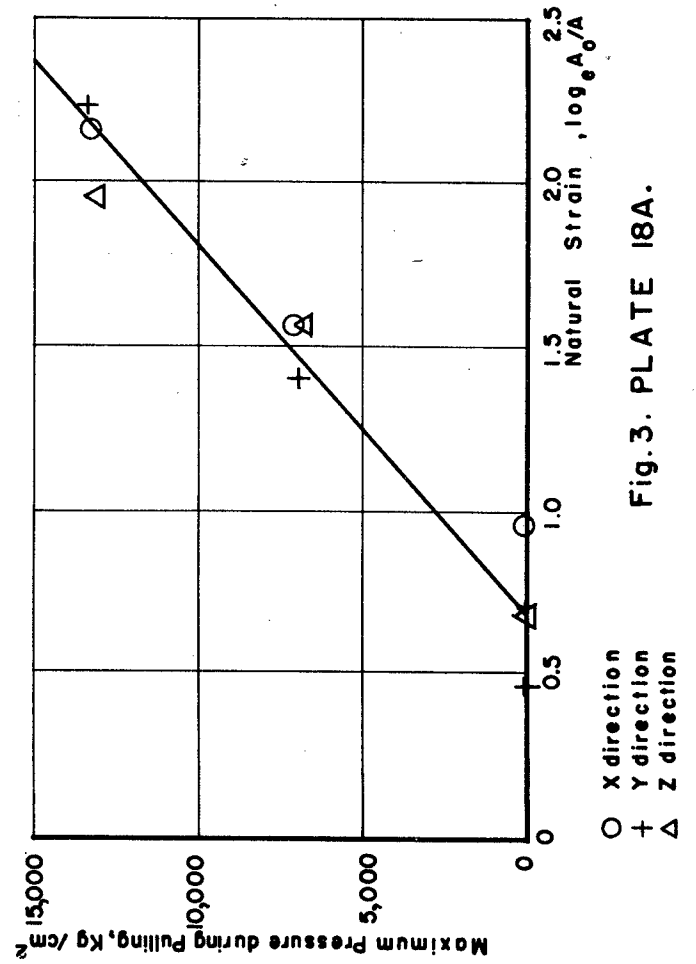


Fig. 3. PLATE 18A.

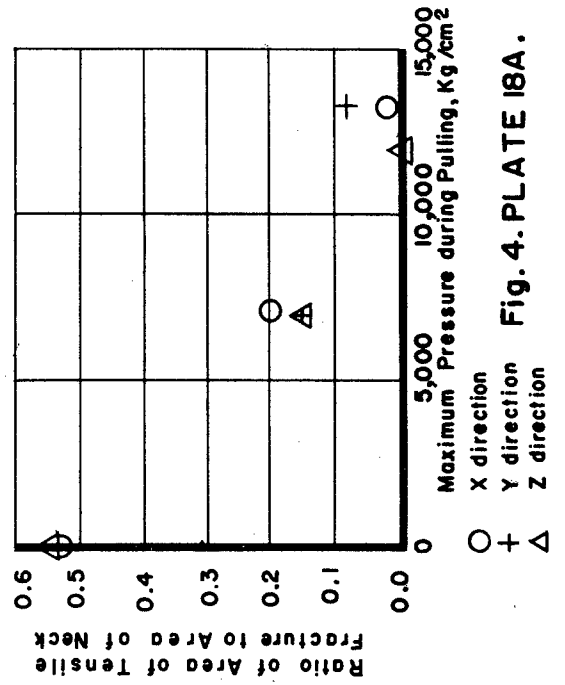


Fig. 4. PLATE 18A.

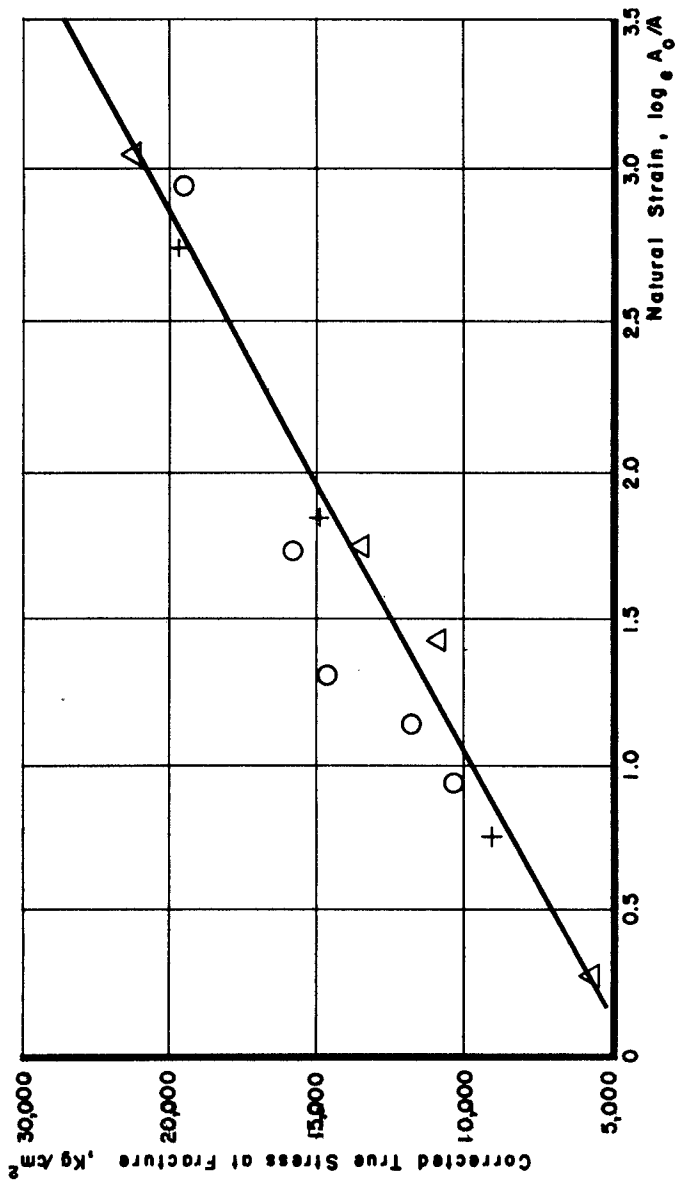


Fig. 5. PLATE 13F.

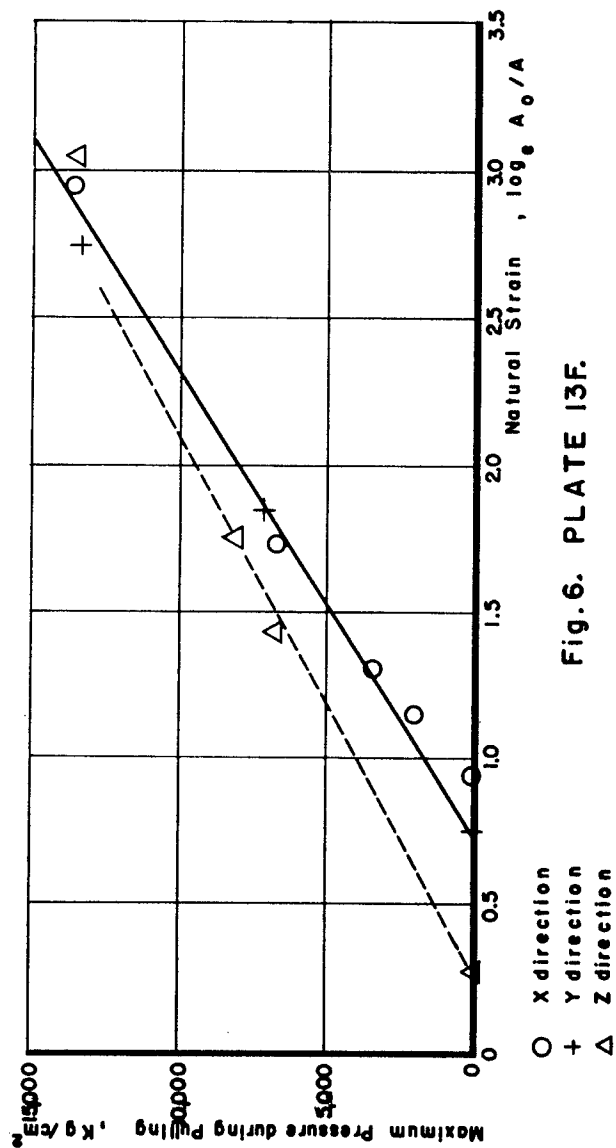


Fig. 6. PLATE 13F.

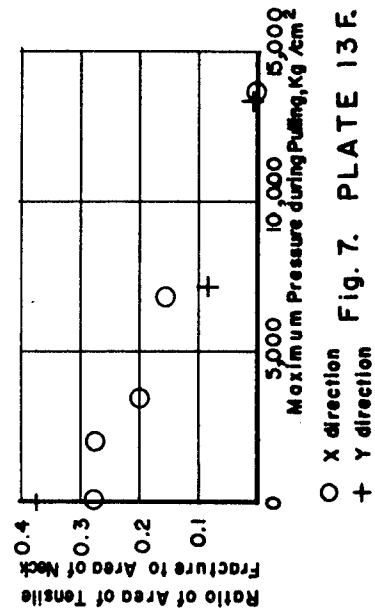


Fig. 7. PLATE 13F.

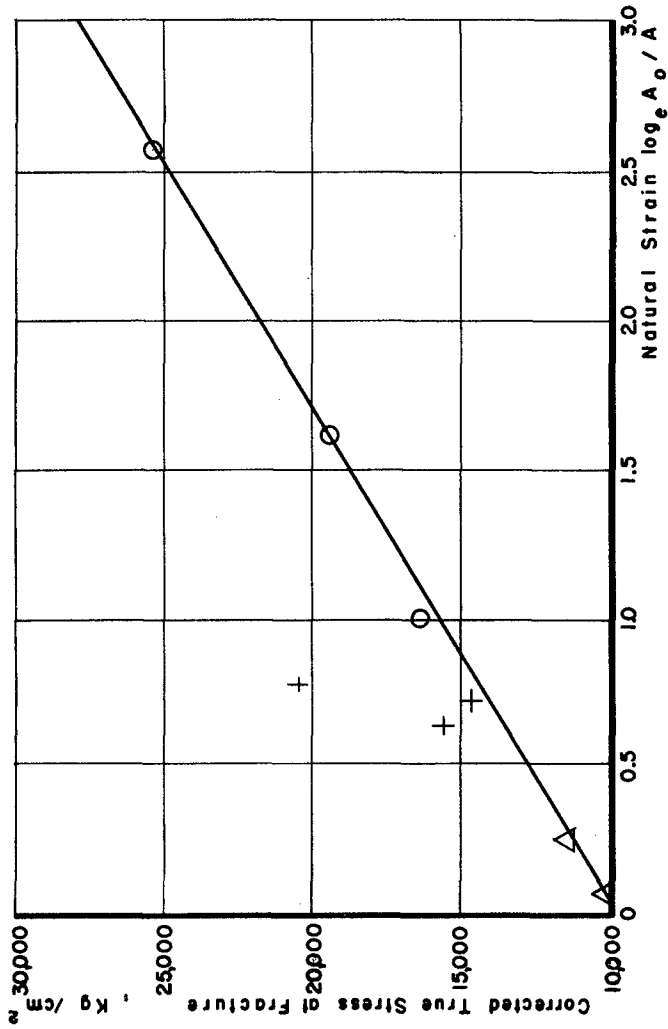


Fig. 8. PLATE 17F.

○ X direction  
+ Y direction  
△ Z direction

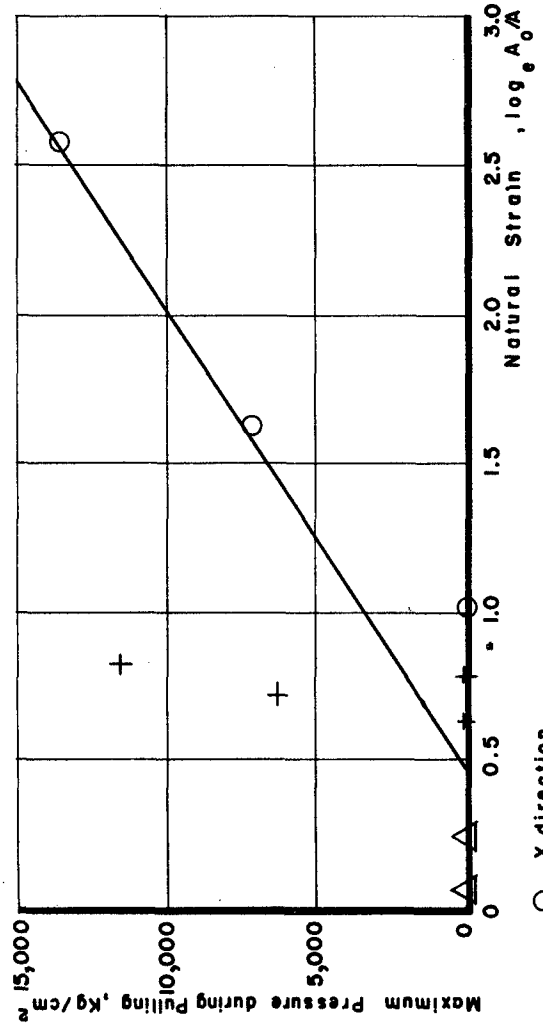
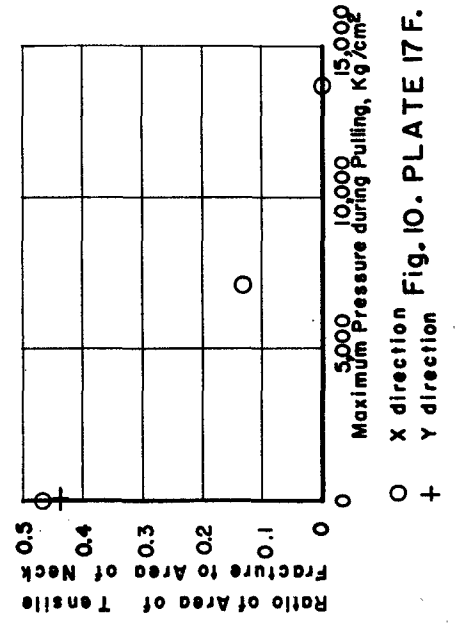


Fig. 9. PLATE 17F.

○ X direction  
+ Y direction  
△ Z direction



○ X direction  
+ Y direction



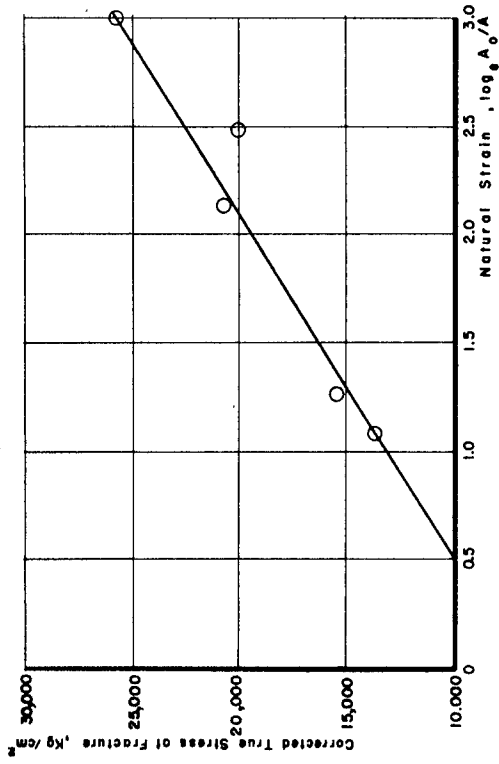


Fig. 11. PLATE 6X 1.

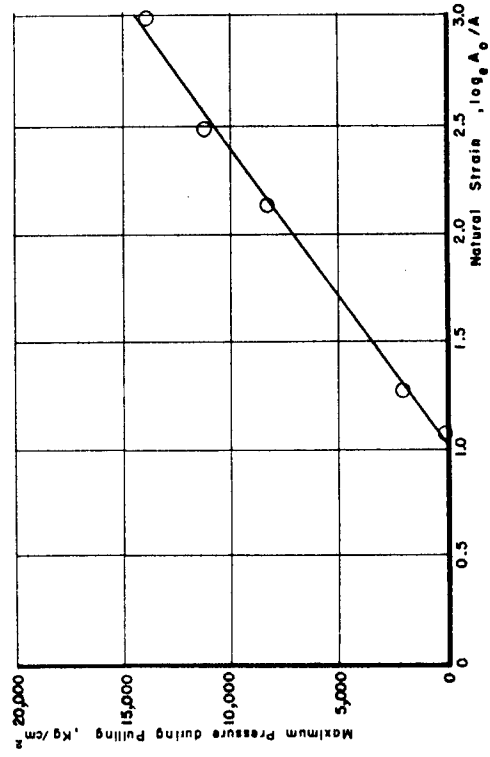


Fig. 12. PLATE 6X 1.

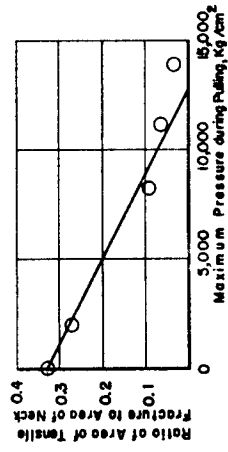


Fig. 13. PLATE 6X 1.

which was pulled at a pressure of 11,000 kg/cm<sup>2</sup>. In the course of the experiment it was thought from the nature of the results that the specimen had been pulled to fracture; but, on opening the apparatus, separation was found to be incomplete, an axial section through the neck having the appearance indicated in Fig. 14 -- an open channel through the center with two isthmuses on either side. This configuration would appear to be the result of a combination of high ductility in the sound parts of the metal, imparted by the pressure, and of strongly segregated impurities, nonductile and probably nonmetallic, such as slag. The location of the inclusions is such as to show up most strongly for specimens with the Z-orientation, but the effect of their presence may be seen also in the fractures of the X-orientation. The shearing part of these fractures never showed the clean-cut slip planes characteristic of sound metal, but the surfaces of shearing slip were dotted with minute pits, giving a matt appearance.

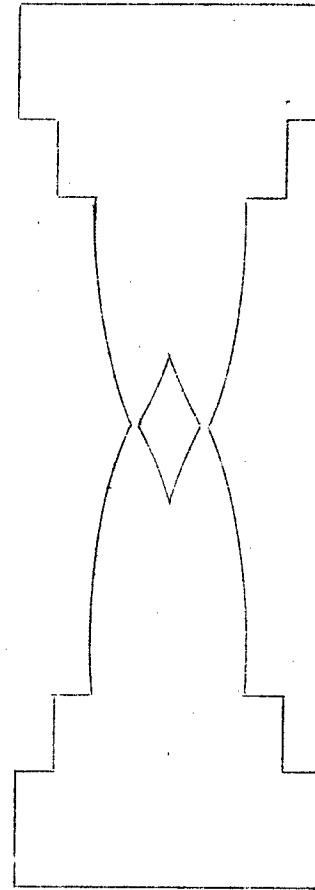


Fig. 14. Double neck on a tension specimen from plate 17F.

The pressure at which the shearing fracture disappears is distinctly lower for the X-orientation of plate 13F than for the other two.

In homogeneous plate this may be a significant feature, because one might expect that the total energy to produce fracture would be greater in a material in which the tensile -- that is, the brittle -- fracture disappears at low compressive stress. This would indicate that plate 13F should be better ballistically than.

the other two. However, other disturbing effects arising from lack of homogeneity would appear to be so great as to mask any effects of this kind.

In studying the effect of pressure in changing the character of the fracture a number of photographs have been made of longitudinal sections through the tensile specimens of two of the plates of the second report. The section was made by machining away half the specimen. For convenience in machining and mounting for photographing, the second shoulder of the specimen was first machined off. Figure 15 shows one of the sectioned specimens mounted for photographing. Figures 16, 17, 18 and 19 are enlarged views of the neighborhood of the fracture for four specimens from plate C14 which had been ruptured at pressures of 1 atm, 4,000, 10,000 and 15,000 kg/cm<sup>2</sup>, respectively. These show in the first place the progressively greater reduction of area as the pressure at which the fracture occurs increases -- that is, the increase of ductility with increasing pressure. In the second place, the change in the character of the fracture is clearly shown. The "tensile" part of the fracture is the approximately plane surface perpendicular to the axis; this progressively diminishes in extent, both absolutely and relatively, with increasing pressure, until at 15,800 kg/cm<sup>2</sup> it has entirely disappeared and the fracture is all "shearing" in character, with a multiple cone of shear at the center. It is especially to be noticed that the tensile part of the break is situated at the smallest part of the neck, whereas the shear runs into the outer surface where the neck is larger.

## 5. Conclusion

The final conclusion to be drawn from these measurements, as far as ballistic applications are concerned, is one which, if it had been anticipated, would probably have made unnecessary the method of attack of this paper. The present measurements disclose ample reason for the difference in ballistic behavior of the different plates, but this difference does not depend on anything

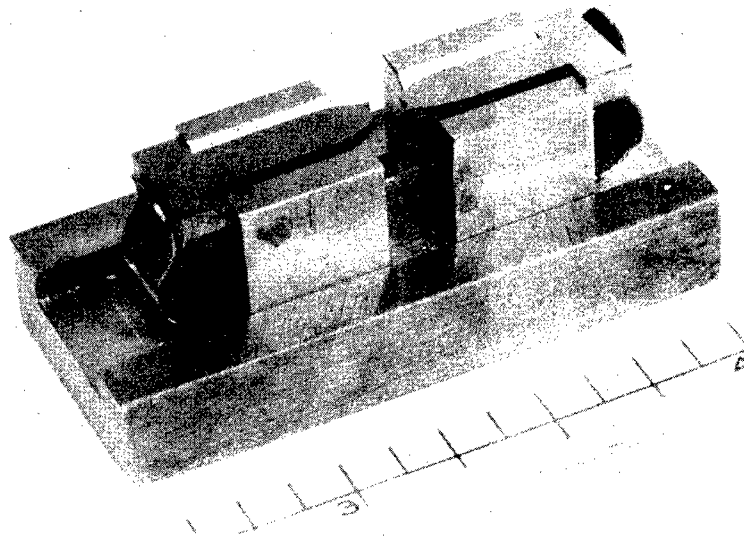


Fig. 15. Showing the method of sectioning a tension specimen. The scale is in inches.



Fig. 16. Specimen from plate C14 broken in tension under atmospheric pressure.

as subtle as a difference in the effects of hydrostatic pressure on the physical properties. Rather, it depends on lack of homogeneity due to large scale inclusions, the effect of which can be adequately shown by tensile tests under ordinary conditions at atmospheric pressure on specimens cut in different orientations. In other words, the bad plates are simply to be described as made from "dirty" steels. This seems to be the conclusion that is also being arrived at from other lines of evidence. It does not follow of necessity that all dirty steels will give plates of bad ballistic properties; but, on the other hand, if a plate is bad ballistically it is pretty likely to be made of a dirty steel, in the absence of such obvious characteristics as too brittle a temper, and so forth.

These present experiments show that the effect of pressure in increasing ductility carries over to dirty steels. The effect is differential; the ductility of the sound part of the metal is increased more than that of the inclusions so that the apparent inhomogeneity may be increased by hydrostatic pressure. A natural expectation would be that fractures in plates made of dirty steels would be initiated at points closer to the projectile than in plates of sounder steels.